

Chemically Etched Silicon Nanowires as Anodes for Lithium-Ion Batteries

Hannah West

*Department of Chemical and Biological Engineering, University of New Mexico, Albuquerque, NM
Power Sources R&D, Sandia National Laboratories, Albuquerque, NM*

Abstract

This study focused on silicon as a high capacity replacement anode for Lithium-ion batteries. The challenge of silicon is that it expands ~270% upon lithium insertion which causes particles of silicon to fracture, causing the capacity to fade rapidly. To account for this expansion chemically etched silicon nanowires from the University of Maine were studied as anodes. They were built into electrochemical half-cells and cycled continuously to measure the capacity and capacity fade.

Introduction

A battery is a device that converts chemical energy into electrical energy. The electrochemical units that comprise a battery are referred to as cells and can be connected in series, parallel or both depending on the desired voltage and capacity output. A single electrochemical cell consists mainly of a negative electrode, a positive electrode and an electrolyte.

The negative and positive electrodes are more commonly referred to as the anode and cathode, respectively. These terms correspond to an oxidation or reduction reaction occurring on the surface. However, it should be noted that this terminology only holds true for the discharge condition of the cell; the electrode assignment is reversed in the charge condition. The discharge condition is most commonly studied as it is associated with a negative Gibbs free energy.¹

Figure 1 describes the motion of electrons and ions during the discharge and charge conditions. While the anode and cathode are always oxidized and reduced,

respectively, their assignment changes depending on the condition of the cell.

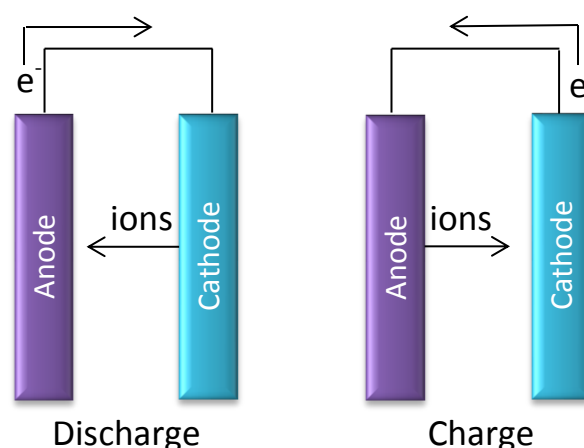


Figure 1: Motion of electrons and ions during discharge and charge conditions of the cell.

The cell also contains a porous polypropylene or polyethylene separator which acts as a mechanical barrier to prevent electrical shorting between the electrodes and is saturated with electrolyte. The electrolyte is a liquid ionic conductor that transfers charge between the anode and cathode. Other components, such as a stainless steel disk and wave spring are

placed inside the cell to create enough pressure on the anode and cathode so that they stay in place after the cell is sealed. The polypropylene gasket on the stainless steel cap facilitates an air tight seal and prevents the cell case from shorting itself. All of the components and their configuration are shown schematically in Figure 2.

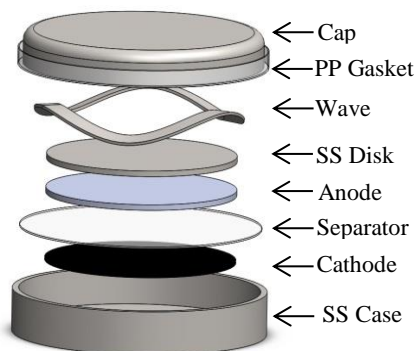


Figure 2: Schematic of electrochemical cell and its components. The cathode and anode are placed on either side of the separator which prevents the components from touching and shorting the cell. The PP gasket on the cap provides an air tight seal and prevents shorting between the cap and case. Electrolyte is applied to the separator to allow ionic charge to transfer between the electrodes.

A cell's capacity is the amount of energy it can store at one time per gram of active (either anode or cathode, whichever is limiting) material and is expressed in milliamp-hours per gram. The theoretical capacity of a cell is specific to the active material that is being used on the working electrode (normally the cathode), which is where the chemistry of interest occurs.² Cells are cycled by moving electrons and ions from one electrode to the other. One cycle consists of charging the cell and discharging the cell. Charging and discharging just refers to which direction the electrons and ions are being transferred. Charging the anode is typically the unfavorable reaction and requires energy to

force it to occur. Discharging the anode is the favorable reaction and releases energy for use in the desired application. There are two types of cycling processes used in the field: galvanostatic and potentiostatic. Galvanostatic cycling applies a constant current and tracks the effect on the voltage while potentiostatic cycling holds a constant potential and measures the current response. Cells rarely reach their theoretical capacity since the ability to move electrons decreases as the cycle proceeds due to lowering of the electromotive force between the electrodes. The actual capacity is determined experimentally by cycling a cell at a current calculated from the theoretical capacity at a very slow rate. The data obtained can be used to find the actual capacity by multiplying the current by the amount of time it took for the discharge cycle to complete. That value is then divided by the amount of material, in grams, of the electrode material under study. This will give the actual capacity in mAh/g.

Background

Lithium-ion batteries are becoming increasingly prevalent as they have many advantages over other battery chemistries. They exhibit high specific energy and energy density. They also have a low self-discharge rate, long cycle life, and can operate in a wide range of temperatures.¹ Currently Li-ion batteries consist of a metal oxide cathode such as lithium cobalt oxide (LiCoO_2) or lithium manganese oxide (LiMn_2O_4) and a carbonaceous anode. Electrode materials with higher specific capacities are required to advance the Li-ion battery as its applications continue to shrink

in size. Silicon is a strong candidate since it has a theoretical capacity roughly 10 times higher than carbonaceous anodes.

LiC_6 has a theoretical capacity of 372 mAh/g while $\text{Li}_{15}\text{Si}_4$, an alloy formed at room temperature and low voltage, has a theoretical capacity of roughly 3,579 mAh/g.^{3,4} This capacity originates from the ability of a single silicon atom to accommodate 4.4 lithium atoms in the crystal lattice. The silicon starts as a single crystalline material, upon lithiation a phase transition occurs forming amorphous silicon. Once the lattice is fully lithiated the material will crystallize into the $\text{Li}_{15}\text{Si}_4$ alloy.³ Unfortunately, silicon has a volume expansion of approximately 270% upon lithiation compared to graphitic anodes which have a volume expansion of approximately 10% upon lithiation.^{3,5} It is speculated that the large volume expansion is due to the transition between the amorphous and crystalline $\text{Li}_{15}\text{Si}_4$. This large volume expansion, combined with the brittle nature of Si, causes the electrode particles to fracture and ultimately leads to a loss of capacity with cycling. This is because the Si shards lose electronic continuity with the electrode and cease to be electrochemically active. While silicon nanostructures experience the same volume expansion as bulk silicon, studies have found that they are able to accommodate the expansion for many more cycles.⁴ Nanowires are the primary nanostructure being researched as viable replacements for carbonaceous anodes. Two methods exist for producing nanowires: (1) epitaxial growth and (2) chemical etching.

Epitaxial Growth of Si Nanowires

The primary method for growing epitaxial nanowires is the vapor-liquid-solid mechanism or VLS. This method is slow and expensive due to the use of metallic impurities such as gold or platinum, high temperatures and a clean environment.⁶ The VLS mechanism utilizes a solid substrate, a liquid impurity and a gas containing the reactive species, in this case silicon. As seen in Figure 3 a droplet of the liquid impurity is placed on the solid substrate while the reactive species gas, silane (SiH_4) for example, surrounds the surface. The crystal lattice forms between the impurity droplet and the substrate due to the highly negative Gibbs free energy in that location. This continues to occur and lifts the droplet away from the substrate. The size of the metallic droplet determines the diameter of the nanowires which are single crystalline and dislocation free.

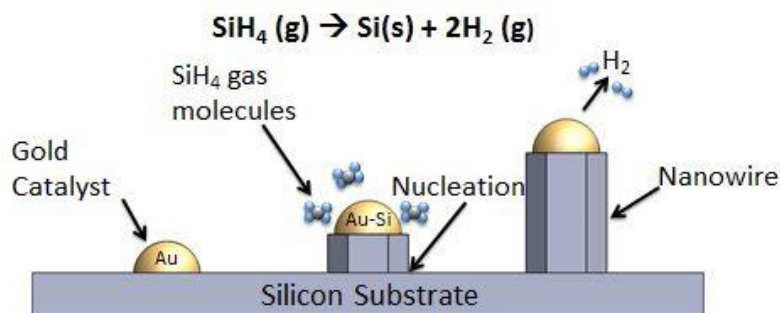


Figure 3: Vapor-Liquid-Solid mechanism for growing epitaxial single crystalline silicon nanowires. The reactive species gas is dissolved into the liquid gold droplet until the droplet becomes supersaturated. Then the silicon will precipitate out and form the crystalline nanowire structure.

Chemical Etching of Si Nanowires

Another technique used to produce nanowires is chemical etching. Etching is accomplished by first removing native oxides with chemicals such as sodium hydroxide or hydrofluoric acid.⁷ A dispersion of metallic nanoparticles such as silver is deposited onto the surface using a number of techniques. The metal nanoparticles are oxidized and the Ag^+ ion reacts locally with silicon to remove it from the surface and etch around the nanoparticle to form a nanowire. This technique creates uniform single crystalline nanowires from the top down and has economic advantages over the VLS method. Reference 7 is a detailed description of two methods for chemically etching silicon nanowires.

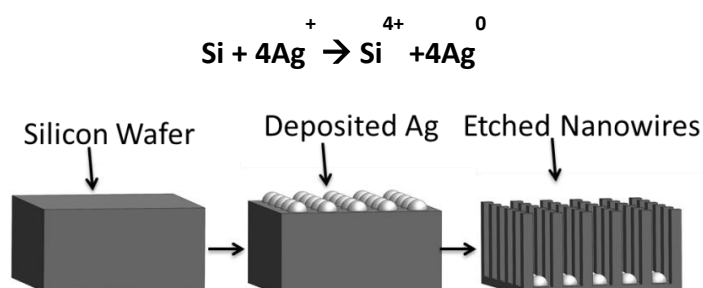


Figure 4: Basic diagram of silver as the metallic catalyst used to etch away silicon from a wafer.

Lithium-ion Half-Cells

Lithium-ion half-cells are used to facilitate the study of silicon electrodes. In a lithium-ion half-cell, lithium metal is used as one of the electrodes. During operation lithium is oxidized which leads to electrons and Li^+ ion transfer to the silicon. In a full cell the lithium metal would be replaced with a metal oxide cathode material. The

lithium metal and silicon configuration is considered a half-cell because it allows only half of the battery chemistry to be studied.

Experimental Methods

Two types of silicon samples were tested for their capacity loss and viability as anode materials. This includes silicon wafers and etched silicon nanowires.

Bulk Silicon

First, bulk silicon wafers were tested as a reference and for establishing a valid test procedure. The wafers were 600-650 μm thick Monsanto silicon wafers doped with phosphorus. Each wafer was broken into squares with an area of about 1-2 cm^2 . The mass and dimensions of each wafer was taken and recorded. These parameters allowed capacity calculations to be performed. Each wafer was “glued” into a stainless steel case in preparation for building a half-cell. The “glue” slurry consisted of 70% DenkaTM compressed acetylene carbon, 30% polyvinylidene fluoride (PVDF) and N-methyl-2-pyrrolidinone (NMP). The acetylene carbon had been baked out in a vacuum oven to remove moisture and compressed for ease of use. PVDF was the binder, NMP was the solvent and the acetylene carbon supplied the electronic conductivity. Silicon is a semiconductor therefore the carbon slurry was needed to ensure that there was enough electronic conductivity to pass charge through the cell. A drop of the slurry was added to a stainless steel case and the silicon wafer was pressed onto the droplet. The cases were allowed to dry overnight in a dry

room and then again in a vacuum oven for 4 hours at 40°C. The drying process was used to drive off as much NMP and H₂O as possible without cracking the slurry. After the drying process was completed the case was ready for assembly.

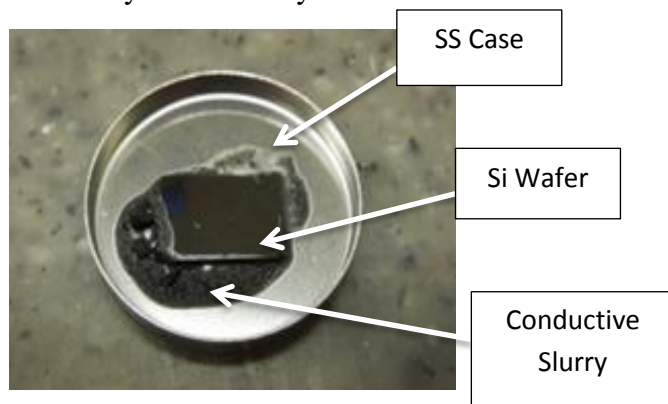


Figure 5. Stainless steel case with silicon wafer “glued” into place. This cell has gone through the drying process and is ready for assembly.

Silicon Nanowires

The nanowire samples were provided by the University of Maine via the second method discussed in reference 7. They were delivered in squares with an area of roughly 1.7 cm² therefore they did not need to be resized for the stainless steel cases. Otherwise, preparation of the silicon nanowire samples for assembly followed the same process as the bulk silicon.

Lithium metal

Lithium metal was the electron source used in these cells and had to be punched into the appropriate size. Lithium metal, 100 μm thick, was punched into .625” diameter electrodes with a hand punch.

Cell Assembly

The preparation of the cases and lithium electrodes were performed in a dry

room that was maintained down to -30°C dew point or drier. The cell components were then brought into a glovebox with an argon atmosphere. The cells were built in this atmosphere to minimize the effects of oxygen and water on the cell chemistry, most importantly lithium. A porous polypropylene separator was placed on top of the electrode in the case. The lithium electrode was scratched to remove any oxides that formed on the surface and then was placed face down on top of the separator. The stainless steel disk and wave spring were stacked on top of the lithium as shown in Figure 2. Once these components were centered in the case, 198 μL of electrolyte was applied to the separator with an Eppendorf pipette. The electrolyte that was used in these cells was 3 parts ethylene carbonate (EC) to 7 parts ethyl methyl carbonate (EMC) with 1.2 molar lithium hexafluorophosphate (LiPF₆). This solution is able to effectively transfer Li⁺ ionic charge between the anode and cathode during cycling. After the addition of the electrolyte the cap was carefully placed over all of the components and the cell was crimped shut onto the polypropylene gasket using a hydraulic press. Each cell was tested with a voltmeter to determine if shorting between Li and the Si or case had occurred.

The carbon slurry used to add conductivity was also helpful when assembling the cells since it held the silicon wafer and nanowires in place. Free standing electrodes are much harder to build into a cell since attention to their location is very important. If the electrodes sit at the edge of the cell the likelihood of them touching and

shorting the cell is much higher.

While this assembly mostly followed standard cell assembly procedures, there were a few minor deviations that should be noted. Typically the cathode material is placed in the stainless steel case. Traditional Li-ion battery cathodes are powders coated onto a current collector, copper or aluminum for example, which supplies enough conductivity for the electronic charge to pass. Since silicon is a semiconductor it must have electronic conductivity added to it by using the carbon “glue”. This could be challenging if the silicon is placed in the typical anodic material location (on top of the separator). In essence, the cells were built backwards compared to standard Li-ion configurations. This can make references to charging and discharging the cell confusing. Therefore, charging refers to the insertion of lithium into silicon and discharging is desorption of lithium into silicon.

Testing Procedure

The cells were labeled, removed from the glovebox and placed in an oven containing a boom box (for safety) and cell holders. Figure 6 is a photograph of this configuration.

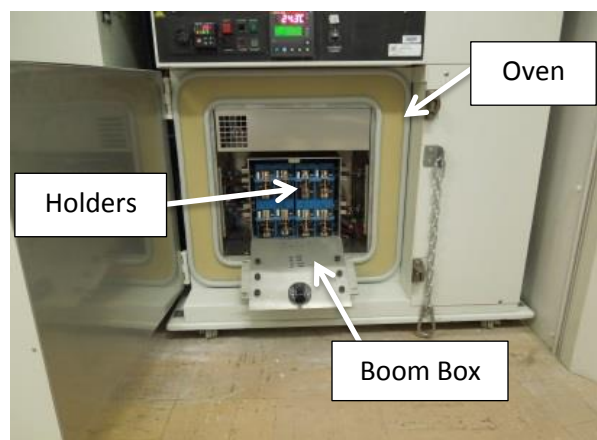


Figure 6. Oven, boom box, and cell holder configuration for cycling cells continuously. Each configuration holds and tests 8 cells independently.

The ovens were set to 25°C and cell cyclers (Maccor Instruments, Tulsa, OK) were programmed to run the cells through varying tests. First, charge-discharge or lithiation-delithiation cycling was performed on these cells. The lithiation-delithiation process for these cells started as galvanostatic. A constant current was applied to lithiate the silicon or move electrons from the lithium metal to the silicon. This was based on a C rate, which is the rate at which a cell discharges relative to its capacity. A rate of 1C requires a current that would discharge the cell in one hour. For these batteries, $1C = 340 \text{ mA/cm}^2$.

The cells were charged (Li inserting into Si) at 0.01C based on the theoretical capacity to a lower limit of 0.01V. They are then discharged at 0.01C (Li extracted from Si) to a voltage of 1.0V, and then held at 1.0V potentiostatically while the current decayed to 0.001C. The cells were run again in a similar manner, but were charged and discharged at a current consistent with a rate of 0.25C based on the actual capacity of the cell. These cells were tested from 0.1V to

1.5V.

Next, cyclic voltammetry (CV) was performed on the wafers and nanowires which identified the voltage at which silicon lithiation and delithiation was occurring. The CV's swept from 0.01V-2.2V at a constant voltage of 0.1 mV and recorded the current throughout that range. The peaks that appeared indicated where lithiation and delithiation was occurring for the silicon sample. Then these voltages were compared to the charge-discharge cycling performed previously.

After these tests the cells were disassembled in a glovebox and the silicon electrodes were analyzed using Scanning Electron Microscopy (SEM) and Energy Dispersive X-ray Spectroscopy (EDS).

The images in Figure 7 are of the silicon nanowires before assembly. The University of Maine reported on similar images claiming that the textured substrate, seen at the bottom of the right image, supports their assumption that the nanowires are porous. Figure 8 also supports this assumption with visible pores appearing in the crevices of the nanowire.

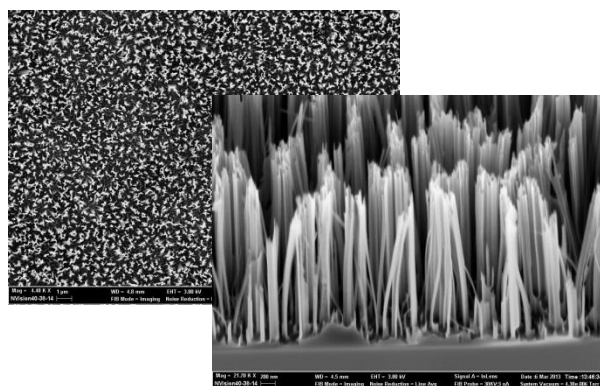


Figure 7. Chemically etched silicon nanowires after production. The textured substrate supports the assumption of porous nanowires.

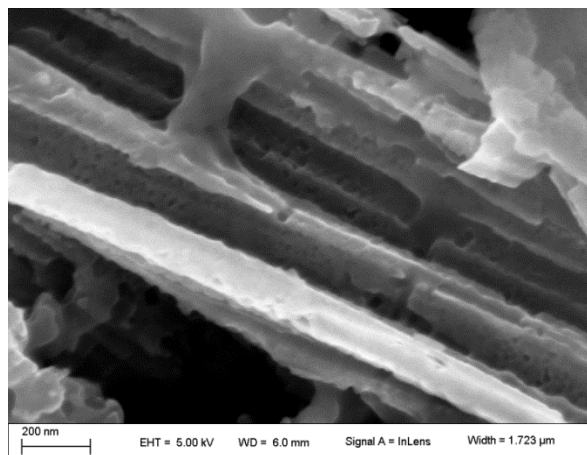


Figure 8. Image of nanowire showing small pores in the ridge, there is also some dried electrolyte present which is expected from a cell that is immersed in the liquid and not washed off before examination.

Porous nanowires increase the surface area available for radial diffusion. This can aid the chemistry occurring in the cell and improve capacity as well.

Results and Discussion

Cyclic voltammograms (CV) were used to identify the voltages at which silicon lithiation and delithiation occurred for the silicon wafers and the silicon nanowires. These two samples have slightly different voltages for lithiation vs. delithiation which is likely due to different phase transitions. Cyclic voltammograms are potentiostatic cycling techniques that sweep across a voltage range and measure the current response. They are useful tools for ensuring that the expected chemistries are occurring.

Typical cyclic voltammograms have definitive peaks and do not exhibit plateaus as seen in the wafer data. The electrometer used reaches compliance at 5V therefore it wasn't able to deliver enough voltage to

meet the current requirement which caused the plateaus.

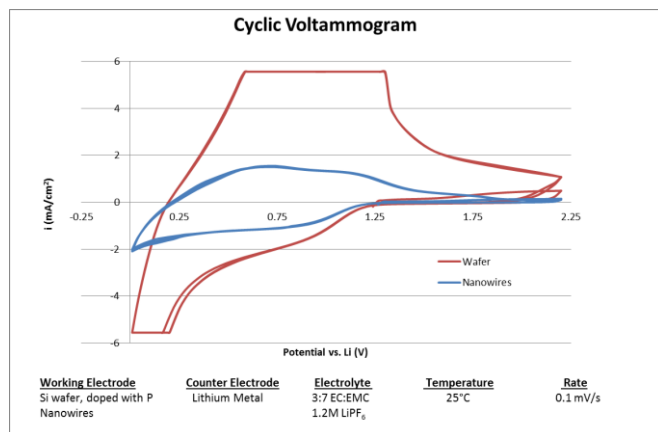


Figure 9. Cyclic voltammograms for silicon wafer and silicon nanowires. The cells are identical except for the working electrode composition.

The cyclic voltammograms were run after charging and discharging the cells. This could have affected the results since there are stabilization events occurring in the first few cycles. It is also likely that the charge-discharge cycles damaged the samples which would change the reaction of the current. Also the cyclic voltammograms might exhibit more definitive peaks at slower rates. A slower rate of cycling allows for the (possibly slow) kinetics at the surface electrode of the reaction to occur more completely.

Figure 10 shows a cyclic voltammogram of a silicon wafer tested initially. While this cannot be compared directly to the current samples since some assembly procedures have been modified, it is a good example of what we would expect to see in a CV. This was run at a much slower rate and prior to charge-discharge

cycling, both of which affect the shape and currents in a CV curve.

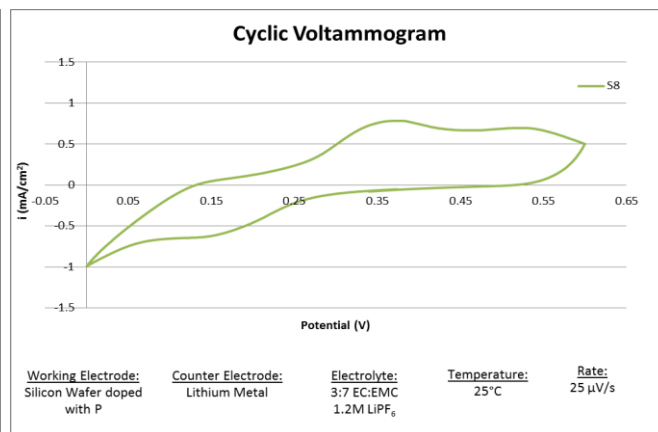


Figure 10. Cyclic voltammogram showing peaks for lithiation and delithiation at 0.4V and 0.15V, respectively.

The first charge-discharge cycles were ran at a rate of 0.01C relative to the theoretical capacity. This actually resulted in a much faster rate since none of the samples were close to reaching the theoretical value. Each cell was cycled one time; however this alone is not a good measure of cell performance since many factors play a role in the capacity loss during the first few cycles. One major factor is the formation of a solid electrolyte interphase (SEI) during the first few cycles. The SEI is a passive layer that helps to prevent further electrolyte degradation by providing a resistive element to the electrode, raising the potential which the electrolyte experiences, but still allows ions to pass through.⁸

Silicon composites were also cycled this way to test whether silicon works with the chemistry necessary to use a Li-ion battery. The composite is a high surface area electrode composed of silicon powder, acetylene carbon and PVDF coated onto

carbon-coated aluminum. The composite electrode resembles the graphitic anode traditionally used in Li-ion batteries more accurately than the wafers and nanowires. A discharge curve that is similar to typical Li-ion batteries is sufficient to confirm silicon's ability to act as an electrode material. The curve below exhibits a form similar enough to traditional discharge curves to confirm that silicon will work with this chemistry. The composite exhibits a lower capacity, but that is expected.

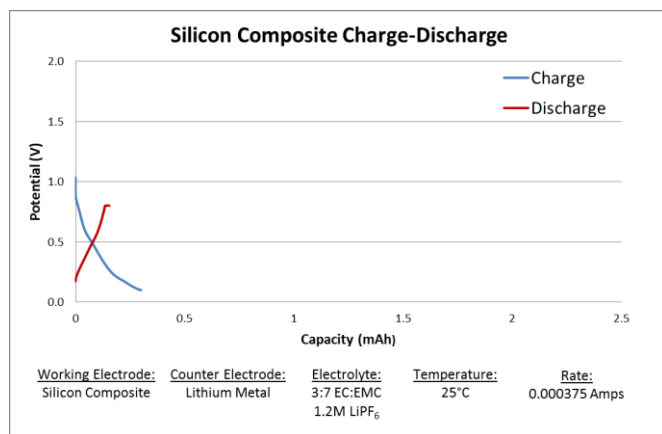


Figure 11. Charge-discharge curve for silicon composite to confirm that silicon works with Li-ion chemical reactions. The form is similar enough to claim that silicon works with the chemistry inside the cell.

The charge-discharge curves give us a general form for the wafers and nanowires, but the capacity loss and Coulombic efficiency calculated from the first cycle are not accurate. The nanowires experienced a 68.5% capacity loss on the first cycle while the bulk silicon samples experienced an average capacity loss of 80.2% on the first cycle. These values are much higher than the capacity loss seen in later cycles. Figure 12 shows the plots for both samples.

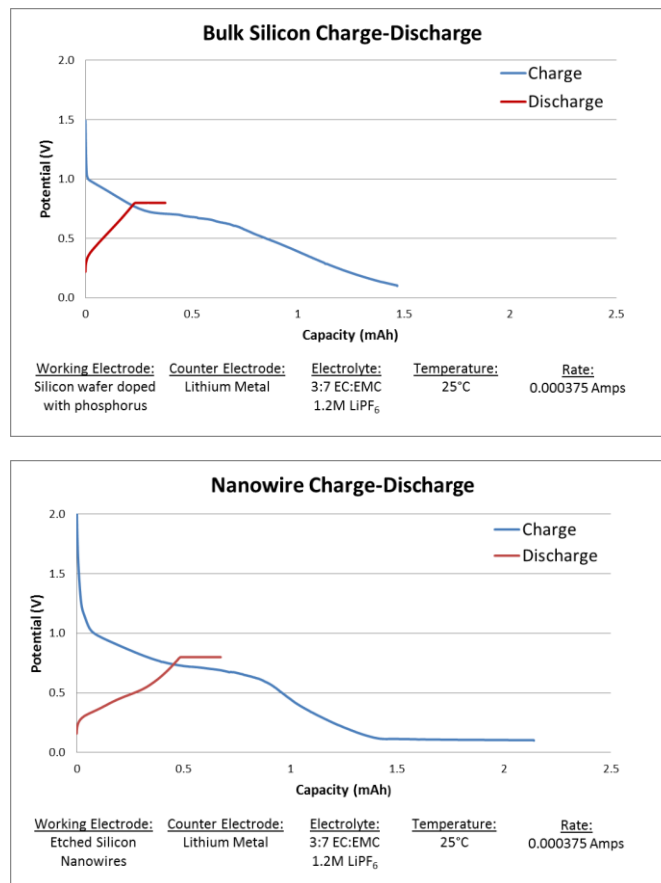


Figure 12. Charge-discharge curves for cells run at 0.01C relative to the theoretical capacity. These plots do not give accurate information on Coulombic efficiency or capacity loss since the first cycle typically involves an SEI formation and the reaction is trying to stabilize.

Typically, cells are tested at their theoretical capacity for 5-10 cycles. This allows the SEI to form and the chemistry to stabilize in the cell. The final discharge cycle is then used to calculate the actual capacity of the cell. This gives a fairly accurate value of the actual capacity and allows different rates to be run for various numbers of cycles. Since only one cycle was run on these cells the actual capacity estimation was not correct. The cells ran for roughly 95 hours on the charge cycle when

the expected discharge time was 10 hours. This indicated that the initial estimate of the actual capacity from the first cycle was not accurate. The cells were cycled again at 0.1C, but with a current that was 10 times greater than the original estimated value (0.306 mA for the wafers and 0.582 mA for nanowires). This resulted in a C rate close to 0.25C. The cells were run at this rate for 5 cycles and then the capacity loss and Coulombic efficiency were determined. The silicon wafers had an initial capacity loss of 38% which decreased to 5.3% the following cycle and continued to decrease until reaching 3.7% on the fifth cycle. The Coulombic efficiency was roughly 99.6%. Coulombic efficiency is the measure of how reversible the reaction is. Copper plating and stripping on gold is 100% efficient since all of the material plated is also stripped during the reverse reaction.⁹ An efficiency of 99.6% for bulk silicon was expected since it is not a completely reversible reaction. The nanowires had a capacity loss of about 3% across the cycles and a Coulombic efficiency of 97.7%. This efficiency is low, but that is expected in low cycle numbers since the SEI is forming and consuming electrons and ions. It is possible that with higher cycle numbers the efficiency will increase as long as the SEI has finished forming. There is also a bulk silicon wafer at the bottom of the nanowires. This could be playing a role in the insertion and desertion of lithium atoms which could also affect the Coulombic efficiency. The nanowires are roughly 20 μm tall compared to the overall wafer thickness of 600 μm . This means that there is a possibility that some lithium is inserting into the wafer itself.

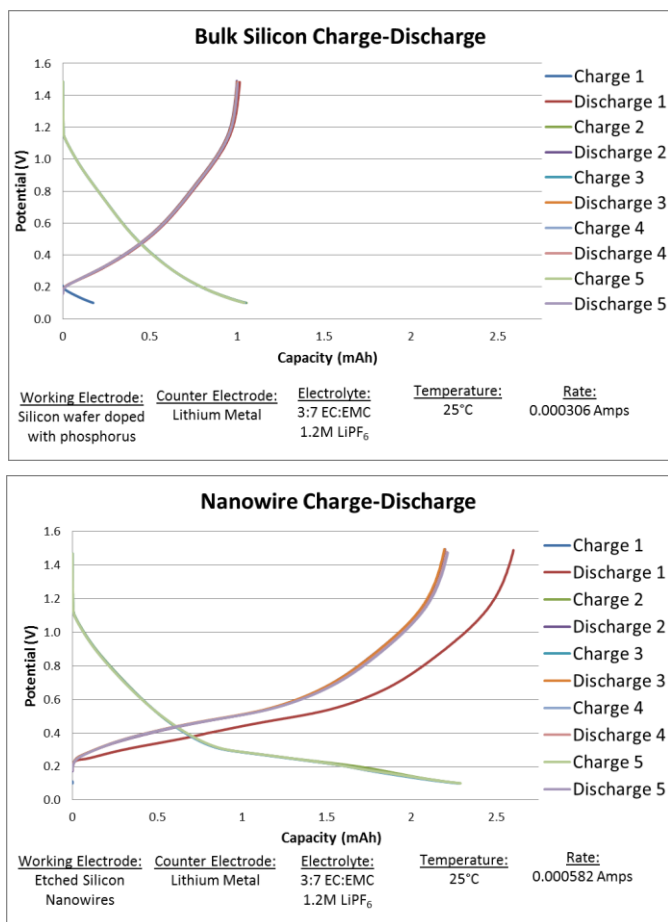


Figure 13. Charge-discharge curves at 0.25C for 5 cycles. These curves do not exhibit the same plateaus from figure 8. It might be necessary to run the cells up to a higher voltage in order to see those features.

The cells were also analyzed using Scanning Electron Microscopy (SEM) with Energy Dispersive X-ray Spectroscopy (EDS). These techniques were used to see how cycling physically affected the silicon electrodes in terms of structure and chemical distribution. Figure 14 shows a silicon wafer control and a wafer after cycling. The effect of silicon's large volume expansion is clear in the cycled wafer. Even without the use of the equipment it was clear that the silicon had been affected because the solid piece of wafer had turned into a fine powder by the Li insertion/removal process.

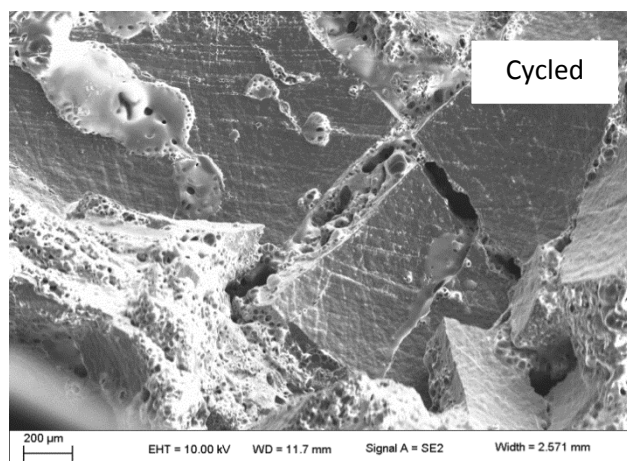
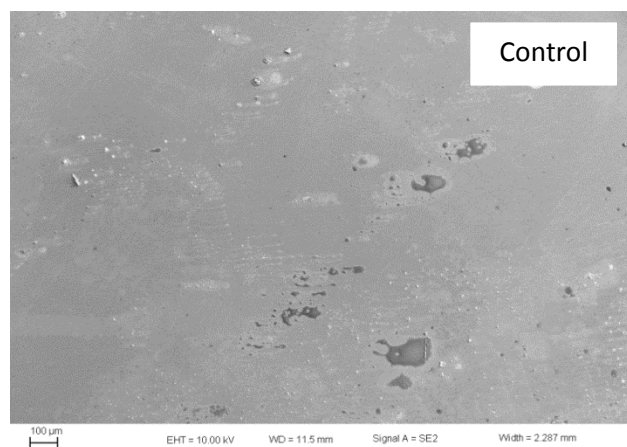


Figure 14. Silicon wafer control sample and cycled sample, both samples were assembled into an electrochemical half-cell and exposed to electrolyte. The wafer is clearly pulverized from insertion and desertion of lithium.

Upon examination with EDS it was clear that the electrolyte had dried in some regions and that there was also an oxide layer that formed either during assembly or transfer into the SEM. Since it was difficult to control for an oxide layer, there is an understanding that its presence could affect the cell performance. There was some research done at the University of Texas claiming that a controlled oxide layer can even enhance the stability of nanostructured silicon.¹⁰ Figure 15 shows EDS results for a region of the wafer.

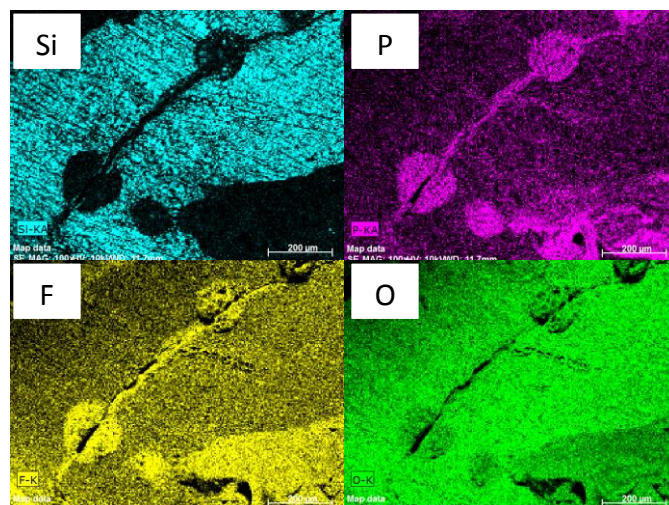
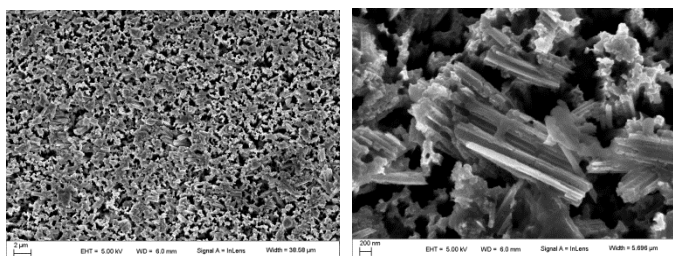


Figure 15. Electron dispersion x-ray spectroscopy images of a crack in the silicon wafer. It is clear that the electrolyte dried in the crack since there is a large concentration of P and F in that region. Oxygen is very prevalent on the whole surface which indicates a uniform oxide layer has formed.

Control



Cycled

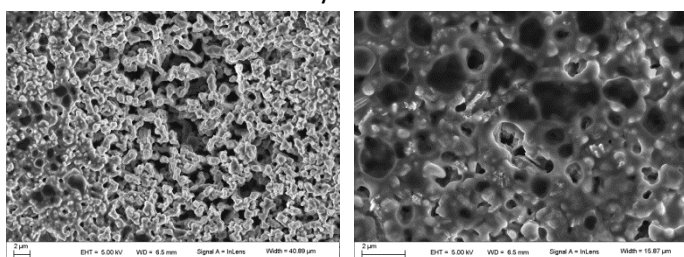


Figure 16. Silicon nanowire control sample and cycled sample. Both samples were assembled into an electrochemical half-cell and exposed to electrolyte.

Figure 16 contains images of non-cycled nanowires and cycled nanowires. It is clear that the electrolyte has an effect on the structure of the nanowires. It is speculated that the electrolyte causes a capillary effect

which pulls the nanowires together and could possibly fracture them. Fracturing of nanowires could have also been caused by pressing on the sample during preparation for analysis in the SEM or during cell assembly due to compression of the cell.

The cycled sample seems to be covered in an SEI layer, which is confirmed with EDS. This could protect the nanowires from the capillary effect by holding them in place. Using a cross sectional examination of the nanowires, it is clear that they are intact underneath the SEI layer that formed above. EDS analysis confirms that the layer above the nanowires does consist of electrolyte components.

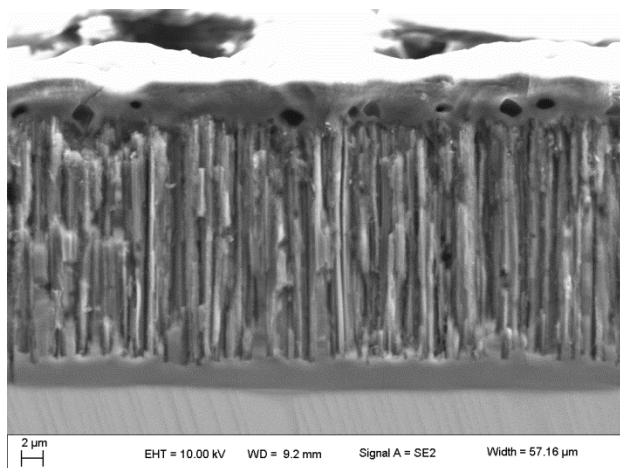


Figure 17. Cycled silicon nanowires covered by a solid electrolyte interphase.

EDS results confirm that the electrolyte is present throughout the samples, but it also reveals that there are silver particles left over from etching and that an oxide layer has formed on the surface. While the presence of silver might produce unwanted side reactions, there is no evidence of Ag/Ag^+ electrochemistry in the discharge curves. The silver is likely in its elemental form which could contribute to some electrolyte degradation. This could be

the cause of a lower Coulombic efficiency since degradation is occurring outside of the SEI formation.

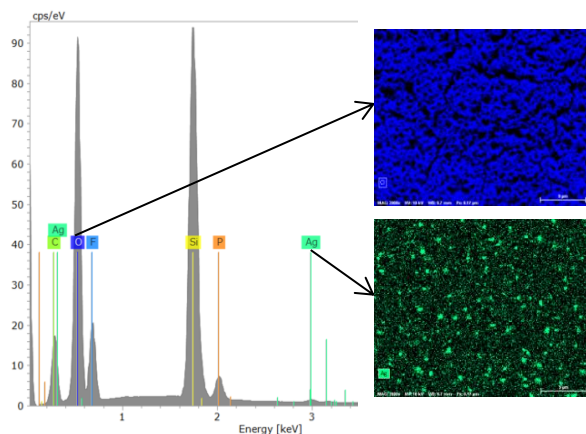


Figure 18. EDS results for cycled silicon nanowires.

Conclusions

The charge-discharge results show that silicon nanowires are viable electrodes and behave similarly to bulk silicon electrodes. Also SEM and EDS analysis prove that the nanowires are able to withstand the assembly process and that an SEI forms within the first few cycles.

To continue this research a new set of cells will need to be built and tested. It is important to label and keep track of each individual cell because knowing the mass will allow for direct comparisons between samples. The cyclic voltammograms will be run first and then the cells will then be charged and discharged at a rate consistent with the theoretical capacity for at least 5 cycles. This will allow the SEI to form and the chemistry to stabilize. Then using the data from the final charge cycle a more accurate capacity can be determined. From there the cells can be tested for many cycles at a rate consistent with the actual capacity. This should give better results for the

nanowires and the bulk silicon to compare to. Thus far the nanowires have been non-uniform. After improving the test procedure uniform samples shall be tested and analyzed to see if there is any improvement from the non-uniform samples.

Acknowledgements

This work was supported by Sandia National Laboratories. I would like to thank Dr. Christopher Apblett, Mrs. Chelsea Snyder, Dr. Brian Perdue and Mr. Jonathan Coleman for their support. I would also like to thank Dr. Scott D. Collins for the etched silicon nanowire samples and Ms. Bonnie Mckenzie for Scanning Electron Microscopy and Electron Dispersive X-ray Spectroscopy of selected samples.

References

- (1) Dahn, J.; Ehrlich, G.; Reddy, T.; McGraw Hill, New York: 2011.
- (2) Bard, A. J.; Faulkner, L. R. *Electrochemical methods: fundamentals and applications*; Wiley New York, 1980; Vol. 2.
- (3) Beattie, S. D.; Larcher, D.; Morcrette, M.; Simon, B.; Tarascon, J. M. *J. Electrochem. Soc.* **2008**, *155*, A158.
- (4) Hatchard, T. D.; Dahn, J. R. *J. Electrochem. Soc.* **2004**, *151*, A838.
- (5) Koyama, Y.; Chin, T. E.; Rhyner, U.; Holman, R. K.; Hall, S. R.; Chiang, Y. M. *Adv. Funct. Mater.* **2006**, *16*, 492.
- (6) Wagner, R. S.; Ellis, W. C. *Appl. Phys. Lett.* **1964**, *4*, 89.
- (7) Smith, Z. R.; Smith, R. L.; Collins, S. D. *Electrochim. Acta* **2013**, *92*, 139.
- (8) Verma, P.; Maire, P.; Novák, P. *Electrochim. Acta* **2010**, *55*, 6332.
- (9) Creutz, H.-G.; Herr, R. W.; Google Patents: 1978.
- (10) Abel, P. R.; Lin, Y. M.; Celio, H.; Heller, A.; Mullins, C. B. *ACS Nano* **2012**, *6*, 2506.



Sandia National Laboratories is a multi-program laboratory managed and operated by Sandia Corporation, a wholly owned subsidiary of Lockheed Martin Corporation, for the U.S. Department of Energy's National Nuclear Security Administration under contract DE-AC04-94AL85000.